PRACTICAL USE OF ROTORDYNAMIC ANALYSIS TO CORRECT A VERTICAL LONG SHAFT PUMP'S WHIRL PROBLEM

by

Mark A. Corbo

President and Chief Engineer

No Bull Engineering

Guilderland, New York

David B. Stefanko

Principal Engineer

and

Robert A. Leishear

Senior Engineer

Westinghouse Savannah River Company

Aiken, South Carolina

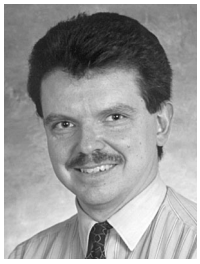

Mark A. Corbo is President and Chief Engineer of No Bull Engineering, a high technology engineering consulting firm, located in Guilderland, New York. He is responsible for rotating equipment consulting services in the forms of engineering design and analysis, troubleshooting, and third-party design audits. Before beginning his consulting career at MTI in 1995, he spent 12 years in the aerospace industry designing pumps, valves, and controls for gas turbine engines. His expertise includes rotordynamics, fluid-film journal and thrust bearings, hydraulic and pneumatic flow analysis, CFD, FEA, dynamic simulations, and mechanical design.

Mr. Corbo has B.S. and M.S. degrees (Mechanical Engineering) from Rensselaer Polytechnic Institute. He is a registered Professional Engineer in the State of New York, and is a member of ASME, STLE, and The Vibration Institute. He has authored over a dozen technical publications, including one that won the "Best Case Study" award at Bently Nevada's ISCORMA conference in 2001.

David B. Stefanko is a Principal Engineer in the Pump Development Program at Westinghouse Savannah River Corporation, in Aiken, South Carolina. He is currently responsible for modification, vibration analysis, and troubleshooting of long shaft pumps. His previous experiences include project and design engineering.

Mr. Stefanko graduated from West Virginia University with a B.S. degree (Mechanical Engineering) and an M.S. degree (Mechanical Engineering).

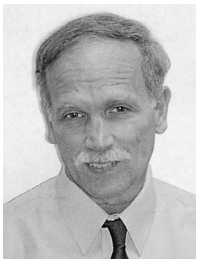

Robert A. Leishear is a Senior Engineer in the Pump Development Program at Westinghouse Savannah River Corporation, in Aiken, South Carolina. He is currently responsible for modifications, process applications, vibration analysis, and troubleshooting of long shaft pumps. His past experience includes design, maintenance/plant engineering, pressure vessel inspections, and process engineering. As part of these tasks he has implemented designs for rotating and reciprocating equipment, control systems, and piping systems.

Mr. Leishear received a B.S. degree (Mechanical Engineering) from Johns-Hopkins University and an M.S. degree (Mechanical Engineering) from the University of South Carolina.

ABSTRACT

The use of long shaft vertical pumps is common practice in the nuclear waste processing industry. Unfortunately, when such pumps employ plain cylindrical journal bearings, they tend to suffer from rotordynamic instability problems due to the inherent lightly-loaded condition that the vertical orientation places on the bearings. This paper describes a case study in which the authors utilized rotordynamic analysis and experimental vibration analysis to diagnose such a problem and designed replacement tilting-pad bearings to solve the problem.

The subject pumps are 45 foot long vertical pumps used for mixing nuclear waste in one million gallon tanks. Each pumping system consists of an induction motor driven by a variable frequency drive, a segmented pump shaft with a centrifugal impeller at the bottom, and a pipe column that surrounds the pump shaft and is suspended into the tank. The column is filled with water that serves as the lubricant for the eight plain cylindrical journal bearings that support the pump shaft.

Unfortunately, these pumps have been plagued with vibration-related problems, such as bearing and seal failures, ever since they were commissioned. In order to evaluate the problem, the pump shaft and column were instrumented with vibration transducers, and vibration testing was performed. This testing revealed that subsynchronous whirling, at approximately one-half the running speed, was the primary culprit responsible for the failures.

In an effort to understand the cause of the observed vibrations, a two-level rotordynamic model of the pump shafting and column was constructed. This rotordynamic model, like those for many vertical pumps, was far from routine. The rotordynamic analysis, which is described in detail, then successfully confirmed that the problem was subsynchronous whirling due to rotordynamic instability. This analysis was then used to guide the design of tilting-pad bearings employing offset pivots and geometric preload to replace the original plain cylindrical bearings and, thereby, resolve the instability problem. The plain cylindrical bearings were removed from a pump, tilting-pad bearings were installed, and subsequent testing verified the predicted vibration reduction. Accordingly, the application of tilting-pad bearings, whose design is described in detail, was conclusively shown to be an effective solution for this specific problem.

INTRODUCTION

Vertical pumps tend to suffer many more rotordynamics problems than do their horizontal counterparts. Common problems experienced in such installations include failed bearings and wiped seals. Accordingly, a thorough lateral rotordynamics analysis should be included as an integral part of the design process for any vertical pump. A comprehensive procedure for performing such an analysis is provided in Corbo and Malanoski (1998).

One of the primary problems that plague vertical pumps is that the prevalent use of plain cylindrical journal bearings in them tends to lead to rotordynamic instability problems. The instability is normally manifested as subsynchronous whirling and can lead to catastrophic events. The primary cause of this problem is that the very light load applied to the plain cylindrical bearings due to the vertical orientation tends to render them unstable.

The fact that lightly-loaded plain cylindrical bearings tend to promote unstable shaft whirling is hardly a recently discovered phenomenon. Newkirk and Taylor (1924) mentioned this effect over 75 years ago. Other early works that discuss this phenomenon include Hagg (1946), Hagg and Warner (1953), Poritsky (1953), Newkirk and Lewis (1956), Hull (1957), Orbeck (1958), and Hori (1959). There are many other references that describe this phenomenon, of which Rentzipis and Sternlicht (1962), Pan and Sternlicht (1963), Mitchell, et al. (1965-66), Lund and Saibel (1967), Tolle and Muster (1969), Jain and Srinivasan (1975), Myrick and Rylander (1976), and Crandall (1982) are only a few. In spite of this wealth of information, it is the authors' experience that most pump manufacturers are not well acquainted with this phenomenon and, as a result, the large majority of them employ plain cylindrical bearings in their vertical pumps.

The case to be discussed involves 45 foot long vertical pumps used for mixing nuclear waste in one million gallon tanks at Westinghouse's Savannah River Site. These mixer pumps are used to mix, or slurry, nuclear waste products contained in the tanks prior to transferring the contents out of the tank for further processing. This pump consists of a number of segmented shafts that are joined together by couplings and are driven by a variable speed induction motor. In actual use, the variable speed feature has been rarely utilized and the pump has been primarily run at a constant speed of 1600 rpm.

The segmented shaft is surrounded by a pipe column that is cantilevered downward from the pump's mounting surface. This column is filled with water, which serves as the lubricant for the eight plain cylindrical journal bearings that support the pump shaft. The pumping element is a centrifugal impeller located at the bottom of the assembly.

In the more than 20 years that these pumps have been in operation, they have been consistently plagued by vibration problems that have led to a multitude of mechanical seal and bearing failures. The average seal life has been on the order of 1000 hours, which translates to less than six weeks of continuous operation. Since this is totally unacceptable, pump vibration testing was performed in an 85 foot diameter by eight foot deep test facility tank in an attempt to better understand the cause of the problems. Data were collected using piezoelectric accelerometers mounted at various locations on the pump column and eddy current proximity probes that measured shaft displacements at a location near the impeller. This testing clearly identified the problem as subsynchronous whirling at approximately 49 percent of the running speed. This is the classic "half-speed whirl" that is driven by the cross-coupling effects that occur in plain cylindrical journal bearings.

In order to better understand the problem and identify potential corrective actions, Westinghouse then hired No Bull Engineering to perform a lateral rotordynamics analysis on the pump. This analysis, which accounted for the pump column's flexibility via employment of a two-level model, confirmed that the pump had a rotordynamic instability problem. The rotordynamic model was then employed to guide the design of tilting-pad bearings to replace the original plain cylindrical bearings. The rotordynamic analysis predicted that the proposed bearing change would completely eliminate the instability problem.

Once the analysis was complete, one of the pumps was made available to compare the vibratory performance of the plain cylindrical bearings with that of the tilting-pad bearings. The pumps were tested in a nonradioactive test facility, where vibration data were collected during pump operation before and after the tilting-pad bearing retrofits were implemented. The tilting-pad bearings were observed to significantly decrease the subsynchronous vibrations that had caused the bearing and seal failures and, consequently, are expected to improve reliability during operation in the waste tank environment. The problem and proposed solution are described in detail in this paper.

PUMP DESCRIPTION

Figures 1 and 2 provide cross-sectional views of the mixer pump, displaying the overall construction and the original plain cylindrical journal bearings. The pumps are installed in the tanks through risers located at various locations on the tank tops. The risers are circular openings in the concrete tops of the waste tanks. These risers may be sealed with removable concrete plugs, or in some cases, sealed with equipment such as slurry pumps. A photograph of the pump lying horizontally on its "cradle" prior to installation into the waste tank is presented in Figure 3. The photo shows the bottom of the pump prior to installation of the impeller.

Referred to as a "long shaft pump" since the shafting connecting the impeller to the motor is approximately 45 feet long, the rotating pump acts as a mixer by drawing the nuclear waste into the pump suction and then discharging a high velocity stream or jet back into the tank waste. The waste stream originates at a low pressure and velocity, and then passes vertically up through a protective screen into the pump casing's suction inlet at the bottom of the pump. The impeller then accelerates the waste through the pump volute and out the two pump discharge nozzles. The jets formed at the nozzles entrain waste as they expand into the tank and either dissolve solid salts or lift sedimented waste, called sludge, from the tank bottom. In either case, the jet impingement on the sludge or salt is the motive force to both initiate mixing and to maintain the slurried material in suspension.

Examination of the figures reveals that the pump shaft is made up of three lineshafts that are connected via couplings. These shafts are driven by the motor shaft via a coupling and extend to the pump impeller at the bottom of the assembly. The pump shafting is surrounded by a stationary structure known as the pump column, which consists of eight interconnected pieces of piping. The top of

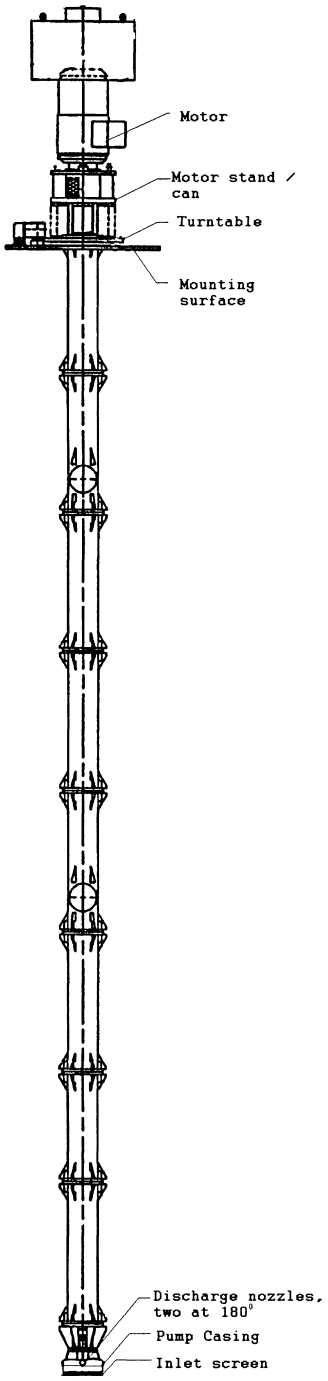

Figure 1. Pump Assembly.

the pump column is attached to the motor stand, which is mounted to the top of a relatively rigid cylindrical can. Since this can is directly mounted to a turntable, the combination of the motor stand and pump column effectively behaves as a cantilevered structure, which hangs down from the point that the motor stand mounts to the can.

At the bottom of each pipe that makes up the pump column lies a flange that holds a plain cylindrical journal bearing. All eight of these bearings are water-lubricated. Additionally, another plain cylindrical journal bearing that is lubricated by the process fluid lies directly above the pump impeller. Since all these bearings are extremely lightly-loaded due to their vertical orientations, they will not generate much of a hydrodynamic film or any significant stiffness or damping. They, therefore, tend to function more as "bumpers" than as hydrodynamic bearings.

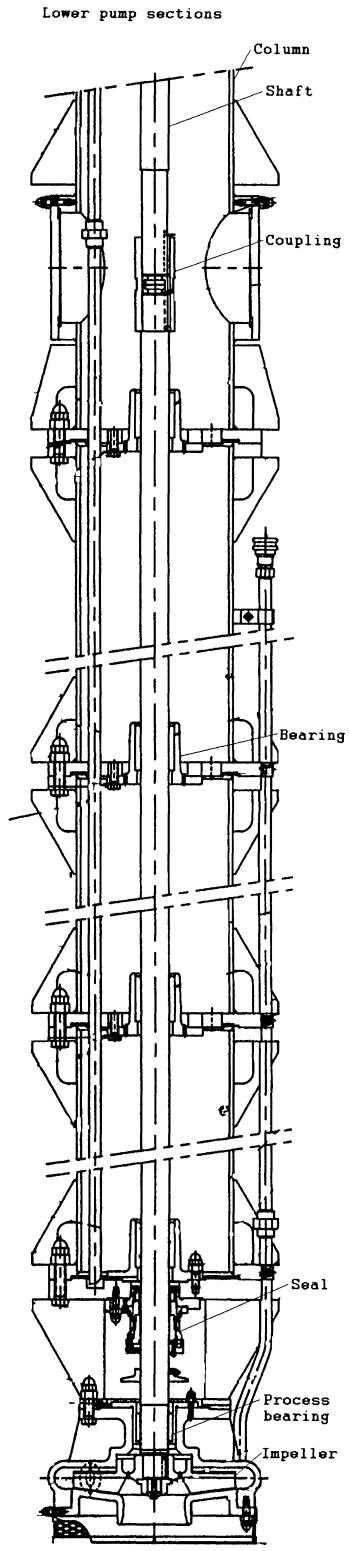

Figure 2. Cross-Section of Pump Assembly.

The pump shaft passes through mechanical seals at both the top and bottom of the pump column to prevent waste escape from the tank through the pump. A dual seal is effectively maintained by pressurizing the corrosion inhibited water that fills the pump column between the two seals. Essentially stagnant in the column, the inhibited water provides the lubricant needed to generate hydrodynamic films in the eight water-lubricated bearings.

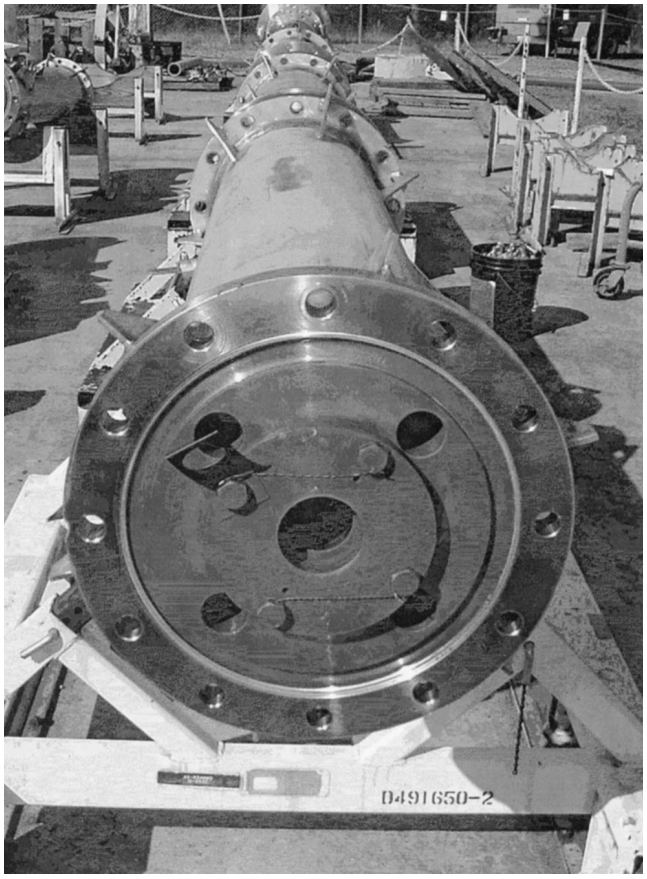

Figure 3. Pump Lying on Cradle.

A rolling-element bearing is enclosed within the mechanical seal at the top of the pump column. The motor thrust bearing (not shown) supports the shaft and impeller weight while the motor stand supports the column and pump casing weight.

The shaft continues from the flexible coupling to the 150 hp motor, operated by a variable frequency drive (VFD). The VFD is capable of operating the pump from 10 percent of full speed to a designed full speed of 1800 rpm. However, due to other considerations, these pumps have been operated as constant speed machines, running at 1600 rpm for virtually their entire lifetimes.

PROBLEM DESCRIPTION

Description of Failure and Problem History

Ever since their commissioning approximately 20 years ago, these long shaft pumps have been consistently plagued by failures directly attributable to high vibrations in the pumping section. These problems occurred in over a dozen units manufactured by each of two vendors. These failures can be primarily divided into two classes—bearing failures and seal failures. Bearing failures refer to failure of the eight water-lubricated plain cylindrical bearings or the process-lubricated bearing that support the pump shaft. These failures appear to be caused by large radial vibrations generating surface-to-surface contact between the journal and bearing surfaces. Evidence of this has been provided by circumferential grooves appearing on various journal surfaces. Figure 4 shows the significant damage that one such journal suffered after only eight hours of operation. In more severe cases of damage, spalling of the bearing surfaces and consequent bearing wear permitted the loosening of small chips, leading to rapid bearing degradation.

On the other hand, seal failures result from overheating. As can be seen from Figure 5, within the seal, a flat annular rotating

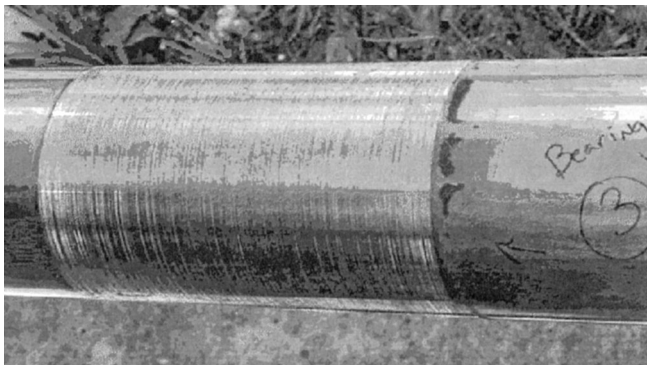

Figure 4. Shaft Damage from Failed Bearing.

surface contacts a mating stationary face. Separated by a fluid film that acts as a barrier seal, one face rotates with the shaft while the other remains stationary. The fluid film is created by pressurizing the water inside the pump column. As the seal rotates, the pressurized water travels radially outward between the seal faces. A radial pressure gradient exists through the water as it travels across the seal face. This pressure gradient prohibits waste migration or diffusion from the tank inward to the pump column. Ideally the water moving across the seal face will evaporate as it approaches the outer edge of the seal due to frictional heat. This evaporation prevents inhibited water from leaking into the tank, making the seal effective in both directions.

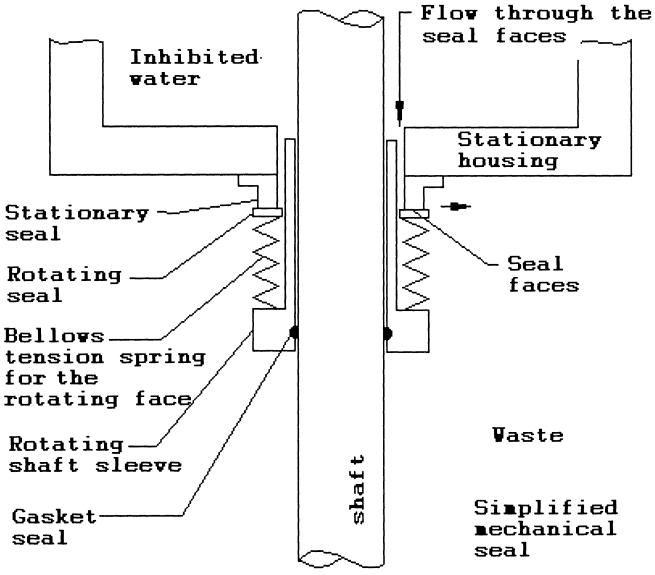

Figure 5. Mechanical Seal Construction.

Excessive vibration increases the friction on the seal surfaces and the available heat for evaporation. Typically separated by distances of 6 to 20 millionths of an inch, the seal surfaces are sensitive to the fluid film between them. Increased evaporation eliminates the film and permits contact between the rotating faces. Thus, larger amounts of vibration lead to more contact, greater resulting surface wear, reduced seal lives, and, consequently, greater leakage rates of water into the tank. Since the goal is to remove the tank contents, not to add inhibited water back into the tank, this represents a significant problem.

Additionally, the two failure modes are not entirely independent of one another. If the bearings are damaged, greater radial shaft motion may be permitted, which increases the vibration across the seal surface with consequent seal wear increase and seal damage.

The seal failure frequency averages approximately 1000 hours, representing less than six weeks of continuous operation. Since this was totally unacceptable from an operations standpoint, a program to measure and analyze the troublesome vibrations, in the hopes of pinpointing their cause and identifying potential corrective actions, was commenced.

Vibration Measurements

In order to measure its vibrations, the pump was installed in a test facility as shown in Figure 6. The pump was mounted to an overhead structural steel platform that spans an 85 foot diameter by eight foot deep tank. Operational vibration readings were obtained with the impeller submerged in water.

Figure 6. Pump Installed in Vibration Test Facility.

To identify the initial pump vibrations, the vibrations were measured via accelerometers at various locations on the pump column and proximity probes aimed at the exposed shaft near the impeller. The results are all presented in cascade or waterfall plots, which are so-named because of their waterfall appearance.

Eddy current proximity probes were used for the shaft measurements. Electrically measuring the changes in resistance between the probes and the shaft as the shaft rotates, these transducers provide continuous measurement of the shaft deflection. Piezoelectric accelerometers were used on the column to measure the force that is proportional to the acceleration. Similar to the crystals used to ignite propane gas cooking grills, these transducers contain a piezoelectric crystal that emits an electrical signal when a force is applied to it. The piezoelectric signals, as well as the eddy current signals, are mathematically interpreted by vibration analysis systems to provide graphic displays of displacement, velocity, and/or acceleration.

The significant number of different vibration frequencies present in the initial vibration signal can be appreciated from inspection of Figures 7 and 8, which represent the waterfall plots generated from the data taken at one of the mid-span accelerometers and at the shaft proximity probes, respectively. The left axis of the plots lists the pump speeds, the lower axis lists the frequencies, and the right axis lists the vibration amplitudes. Inspection of these figures reveals that, at the higher running speeds, significant vibrations occur at several different frequencies—specifically ½×, 1×, 3×, and 5×. Each of these frequencies has specific causes, and understanding the cause of each is critical if one wishes to identify a remedy to reduce that specific vibration.

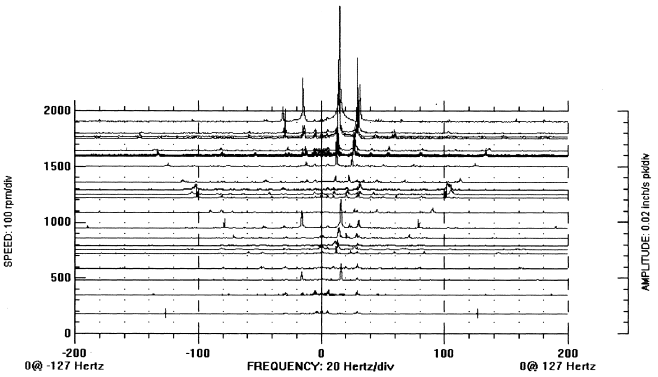

Figure 7. Mid-Span Accelerometer Measured Vibrations for Original System.

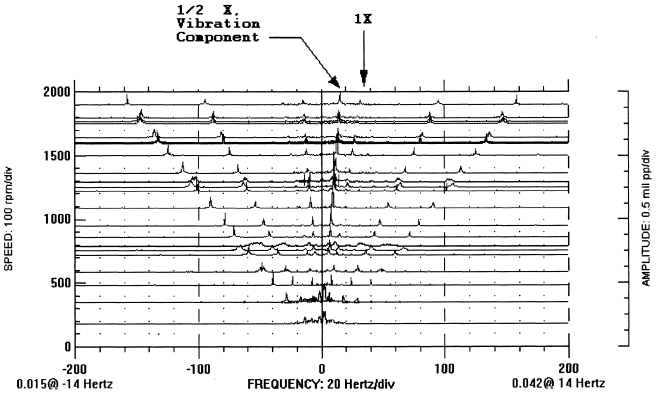

Figure 8. Proximity Probe Measured Vibrations for Original System.

When equipment rotates, vibrations at numerous frequencies are created, and their vibration energies at a point on the machine add together to create the machine's overall vibration spectrum. The first vibration to be considered is referred to as the 1×, or synchronous vibration. The term 1× refers to the fact that the vibration occurs at one times the running speed of the machine. Any unbalance of the shaft, the impeller, or other rotating components directly affects the magnitude of the 1× component. Misalignments can also create 1× radial vibrations, although, unlike unbalance, they are usually also accompanied by axial vibrations. Since all real machines, regardless of how precisely they are balanced and/or aligned, contain some finite amounts of unbalance and misalignment, all machines will have a nonzero 1× component in their vibration spectra.

Looking again at the figures, the ½× frequency represents a subsynchronous vibration that is often referred to as shaft or oil whirl. This means that along with the 1× component already discussed, another slower vibration is superimposed on the shaft. For the long shaft pumps under consideration, the ½× component can be attributed to fluid instability associated with the plain cylindrical journal bearings. An oversimplified explanation for this phenomenon is that the fluid in the journal bearings' clearances carries the shaft along with it at its average circumferential velocity (which is close to ½×).

Other vibrations are also observed to be present in the spectrum, most notably those at 3× and 5×. The 3× component can be attributed to parallel misalignment of the shaft segments at the threaded couplings. In fact, shaft misalignment may result in any combination of the 1×, 2×, and 3× components. However, in this case, the 2× component is negligible. The 5× component is easily identified as being due to blade-passing effects at the impeller since there are five vanes on the impeller.

Once the vibration sources have been identified, their magnitudes need to be considered and acceptable vibration limits need to be defined. In general, determining these limits requires a case-by-case evaluation. Since these pumps' installation in a nuclear environment prohibits any maintenance activities, the amount of vibration that can be allowed must be smaller than for more conventional machines. The typical vibration velocity that the authors use as an index for potential vibration problems for pumps in these types of applications is approximately 0.20 in/sec. This represents the maximum allowable zero-to-peak vibration value. Whenever the observed vibrations exceed this value, pump tests are normally suspended pending vibration evaluation.

Examination of Figure 7 reveals that the ½× component greatly exceeded this limit, with a maximum observed magnitude of about 0.40 in/sec. Accordingly, the high vibrations that were causing the bearing and seal failures were conclusively observed to be subsynchronous vibrations occurring at approximately one-half (actually 0.49×) the running speed. Since lightly-loaded plain cylindrical bearings are a notorious source of these types of vibrations, the authors suspected journal bearing instability as the cause of the vibration problem. Accordingly, a rotordynamics analysis was then performed to attempt to verify this hypothesis.

The only other significant vibration tests that were performed were impact tests on the pump columns. These tests were conducted by striking the column assembly at judiciously selected locations with a heavy plastic hammer and then measuring the frequencies it vibrated at. Using this methodology, the pump column's natural frequencies were observed to occur at 300, 900, and nearly 1800 rpm.

ROTORDYNAMIC MODEL GENERATION

Need for a Two-Level Model

In an effort to, once and for all, pinpoint the cause of the pump's vibration problems, the authors generated a rotordynamic model for the unit. In general, the guidelines provided in Corbo and Malanoski (1998) were employed throughout the entire rotordynamic analysis. In order to accurately simulate the vibrational behavior of all rotating and stationary structures in the unit, a comprehensive model consisting of two independent levels was constructed. The first level represented the rotating pump shaft while the second accounted for the stationary motor stand and pump column.

Each level represents a complete rotordynamic model that simulates the vibratory behavior of the modeled component. The individual levels are linked to each other through "supports" that represent any and all components that tie the vibration of one component to another. Typical supports are bearings, pedestals, seals, and fluid coupling elements. The two-level model allows the complex dynamic interactions that occur between the individual components to be accounted for. Employment of a multilevel model such as this is the only valid way to analyze the rotordynamic behavior of a long, flexible vertical pump such as this one.

The astute reader will note that this multilevel model is significantly more sophisticated than the conventional single-level rotordynamic model, which merely consists of the rotor and its supports. There are two valid methods for constructing these models. The first, and the one normally employed by the authors, is to employ a special rotordynamics code having multilevel capabilities. The second is to construct a rotordynamic model of the rotor and a separate model of the casing using a general-purpose finite element code. If this second option is used, fluid-structure-interaction connections between the rotor and casing must be accounted for using methodologies similar to those given in Childs (1993).

Unfortunately, the authors are acquainted with a number of pump manufacturers who employ the second option but do not attempt to account for the fluid-structure interactions. Such an approach is completely invalid. Pump users should, thereby, be cautioned to check for this very important point whenever they encounter a rotordynamics analysis performed using a general-purpose finite element code.

Although the authors' experience is that the pump community is not well-acquainted with the multilevel analysis techniques described here, there are ample cases in the literature where this approach has been employed in the rotordynamics analysis of vertical pumping systems. These include Berzatzy, et al. (1972), Chang and Braun (1987), Chen, et al. (1978), Childs (1978), Darlow and Smalley (1976), Darlow, et al. (1978), Habets and Smalley (2000), Smalley, et al. (1998a), Smalley, et al. (1998b), and Walter and Zelingher (1989).

General Modeling Procedure Employed

The rotordynamic model is a finite element representation consisting of a series of disk elements interconnected by shaft elements. The disks represent the machine elements having large mass while the shafts behave as flexing springs. The junction points between shaft elements are known as "stations" and are located to correspond to appreciable changes in cross-section, concentrated masses, and bearings.

In general, the rotordynamic model was constructed using the guidelines given in Corbo and Malanoski (1998) and classical techniques. Additionally, the following assumptions and ground rules were utilized:

- For those rotors where it was not given, the transverse mass moment of inertia was assumed to be equal to one-half the polar moment of inertia.
- When modeling regions having abrupt changes in cross-section, the effective stiffness diameter was assumed to grow or shrink along 45 degree lines. The diameter that bisects the 45 degree lines was, thereby, utilized as the effective stiffness diameter. The material outside the stiffness diameter is assumed to add only mass (no stiffness) to the model.
- Since the rotordynamics computer code can only handle axisymmetric elements, the slotted portions of the pump column were modeled as axisymmetric circular sections having the same area and area moment of inertia as the actual cross-sections.
- The flanges on the pump columns were assumed to add only mass (no stiffness) to the model.
- The coupling linking the pump and motor shafts was assumed to be flexible enough such that the two shafts' lateral rotordynamic behaviors are independent. Since all the observed vibration problems were confined to the pump shaft, the motor shaft was not accounted for in the model.
- The concentrated mass and moments of inertia employed for the pump impeller corresponded to the "wet" condition in which the impeller is filled with liquid.
- The threaded couplings that join the lineshaft segments together were assumed to add only mass to the system. Their stiffening effect was conservatively ignored.
- Similarly, since the clearance in the couplings allows the lineshafts to flex independently of one another, the shaft elements at these couplings were assumed to be joined by hinges.

In addition to shaft and disk element parameters, the rotordynamics code was also provided with inputs for the dynamic stiffness and damping coefficients at each support. All eight coefficients were input for the fluid-film journal bearings and hydraulic effects, as will be discussed shortly. However, the action of all other supports was modeled using only the direct radial stiffness coefficients, k_{xx} and k_{yy}, and in some cases, angular stiffness coefficients, k_{bb} and k_{tt}. The cross-coupling stiffness coefficients and all damping coefficients were taken to be zero at these locations.

The following assumptions and ground rules were utilized in the determination of the mechanical stiffnesses used in the model:

- The cylindrical can that the motor stand mounts to was assumed to be rigid and, thereby, directly connected to ground. Accordingly, the entire pump column assembly was treated as if it were suspended from the motor stand mounting flange.
- The angular stiffness of the motor stand mounting flange was calculated using equations for a circular plate, simply-supported at its outer edge, under a trunnion loading.
- Since the motor stand's ball bearing was orders of magnitude stiffer than the pump's plain cylindrical journal bearings, the ball bearing was assumed to be rigid.

Determination of Plain Cylindrical Bearing Coefficients

Once the support stiffnesses were known, attention turned to determining the dynamic coefficients for the nine plain cylindrical journal bearings that supported the pump shaft in the initial configuration. These bearings were modeled using all eight dynamic stiffness and damping coefficients. Unfortunately, the determination of these coefficients was anything but routine. The overwhelming majority of journal bearing analysis codes in existence assume that the fluid film ruptures or cavitates in the diverging portion of the film. Utilization of this assumption makes the calculation of the bearing coefficients a much simpler mathematical exercise. Since at least 99 percent of the world's journal bearings do, indeed, experience rupture, the limitations of utilizing such codes are not usually a problem.

However, the fact that this unit employed plain, ungrooved journal bearings subjected to very light radial loads (due to their vertical orientation) and operated at relatively high absolute pressure levels (due to the pressurization of the pump column) meant that these bearings were operating in the unruptured condition. Accordingly, each of these bearings would have a continuous 360 degree film, which is very bad from a stability standpoint, and which 99 percent of the world's bearing codes are incapable of analyzing.

Fortunately, this condition was not a stopper since the authors have a proprietary code that calculates the performance of fluid-film journal bearings in the unruptured condition. This code calculates the fluid film's pressure distribution for the unruptured condition using a finite difference technique. Since journal bearings in the unruptured state are statically unstable about the centered (zero load) condition, representative radial loads needed to be assumed for each bearing in order to allow the code to generate meaningful stiffness and damping values. The assumptions utilized to calculate these loads were as follows:

- The radial loadings acting on the bottom two journal bearings (the lowest water lubricated bearing and the process-lubricated bearing) were assumed to be entirely due to the impeller's hydraulic radial thrust, which arises from the circumferential asymmetry of the impeller's pressure distribution. The impeller radial thrust was calculated using the Hydraulic Institute procedure for impellers operating within double volute collectors.
- The radial loadings on the top seven journal bearings were calculated assuming that the pump shafts were bowed through a representative straightness tolerance.

Modeling of Pump "Wet" Effects

The combination of the rotordynamic model and the rotordynamic coefficients for the plain cylindrical bearings yields a complete rotordynamic model for the "dry" system. However, as is described fully in Corbo and Malanoski (1998), various hydraulic effects occurring in pumps have a tendency to make a pump's "wet" critical speeds much different from its "dry" values. Furthermore, it has been unequivocally shown that for the vast majority of pumps, the "dry" critical speeds are poor indicators of the unit's rotordynamic behavior during normal "wet" operation. Accordingly, the relevant hydraulic effects were added to the "dry" model to generate the "wet" model, with a corresponding improvement in accuracy.

One of the hydraulic effects that can have a profound impact on a pump's rotordynamic behavior occurs at the interface between the impeller and its surrounding collector. Due to the nonuniform circumferential pressure distribution existing at this interface, hydraulic forces are applied to the rotor whenever the impeller moves away from the centerline. These are modeled using the same stiffness, damping, and mass coefficients that are used to represent the bearings. Unfortunately, prediction of these coefficients is almost impossible to do analytically. Accordingly, empirical methods are the only practical procedures available for doing this at this time.

In his noteworthy rotordynamics textbook, Childs (1993) provides a method for calculating these coefficients using dimensionless stiffness, damping, and mass coefficients that are defined by the following equations:

$$K^* = K / \left(\pi \bullet R_2^2 \bullet b_2 \bullet \rho \bullet \omega^2\right) \tag{1}$$

$$k^* = k / \left(\pi \bullet R_2^2 \bullet b_2 \bullet \rho \bullet \omega^2\right) \tag{2}$$

$$C^* = C / \left(\pi \bullet R_2^2 \bullet b_2 \bullet \rho \bullet \omega\right) \tag{3}$$

$$c^* = c / \left(\pi \bullet R_2^2 \bullet b_2 \bullet \rho \bullet \omega\right) \tag{4}$$

$$M^* = M / \left(\pi \bullet R_2^2 \bullet b_2 \bullet \rho\right) \tag{5}$$

where:
K^* = Normalized direct stiffness coefficient
K = Direct stiffness coefficient (lbf/in)
k^* = Normalized cross-coupling stiffness coefficient
k = Cross-coupling stiffness coefficient (lbf/in)
C^* = Normalized direct damping coefficient
C = Direct damping coefficient (lbf-sec/in)
c^* = Normalized cross-coupled damping coefficient
c = Cross-coupled damping coefficient (lbf-sec/in)
M^* = Normalized mass coefficient
M = Mass coefficient (lbf-sec^2/in)
R_2 = Impeller outside radius (in)
b_2 = Impeller axial width at discharge (in)
ρ = Fluid density (lbf-sec^2/in^4)
ω = Rotational speed (rad/sec)

Worst case nondimensional coefficients for an impeller having this configuration were selected from Childs (1993). Using the above equations, these were then converted into dimensional coefficients that were applied to the model at the impeller location.

The other hydraulic effects requiring modeling were added mass effects at structures immersed in liquid. Added mass effects occur in these locations because when the immersed structure vibrates, it carries some of the surrounding liquid along with it. Accordingly, the effective mass of the vibrating structure is larger than the actual mass

of the component. Per the guidelines of Corbo and Malanoski (1998), the added masses for the rotor were simply assumed to be the mass of the liquid displaced by the volume of the rotor. Using this rule, the added masses were calculated and applied to the rotor model.

The authors normally also use the same displaced volume rule to calculate the mass of liquid that moves along with the vibrating pump column. However, in most of the applications normally encountered, the column is open at the bottom so that water can flow in and out of it when it vibrates. For such a configuration, assuming that only a fraction of the water contained within the column is moving along with it is perfectly legitimate. However, in this application, the column is sealed and pressurized so that all the contained water is forced to move with the casing whenever it vibrates. Accordingly, it was decided to assume that the entire mass of water contained within the column moves right along with the column.

ROTORDYNAMIC ANALYSIS OF PUMP WITH PLAIN CYLINDRICAL BEARINGS

Undamped Critical Speed Analysis

Generation of the added masses represented the culmination of the rotordynamic model-building process. Once the two-level model was complete, it was used to perform a rotordynamics study on the initial system consisting of undamped critical speed and stability analyses.

The first analysis executed was the undamped critical speed analysis. The plain cylindrical bearing coefficients for the 1600 rpm operating speed were input to the rotordynamics code and undamped natural frequency analysis was run. Since fluid-film journal bearings often have significantly different stiffnesses in the y (direction of load) and x-directions, this analysis is normally run twice and two sets of critical speeds, one for each direction, are generated. However, since both the x and y-direction direct stiffnesses were observed to be negligibly small for the plain cylindrical bearings, only one set of critical speeds was calculated.

The undamped critical speeds calculated in this manner were found to occur at 55, 257, 328, 382, 493, 580, 861, 1056, 1255, 1653, 1911, and 1980 rpm. Mode shapes for the first two modes are provided in Figures 9 and 10. Both the figures show the calculated critical speed along with its corresponding mode shape, which shows the normalized displacement as a function of axial position. In these, and all other mode and deflected shapes to follow, the motions of the rotor (level 1) and casing (level 2) are both shown. Additionally, please note that the left-hand side of the figures corresponds to the top of the model and the right-hand side corresponds to the location of the pump impeller.

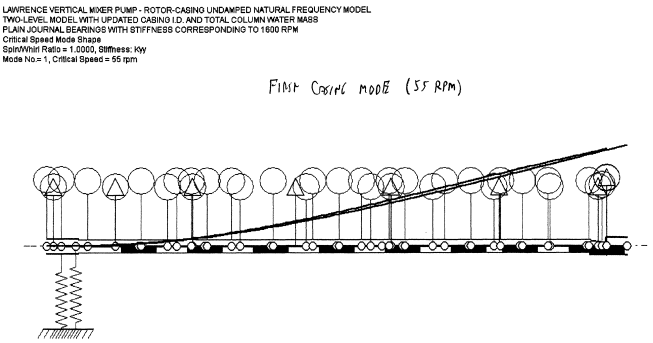

Figure 9. First Casing Mode (55 rpm) with Plain Cylindrical Bearings.

Examination of the undamped analysis results leads to several general conclusions, as follows:

- The undamped modes can all be separated into one of two major classes—rotor modes and casing modes. Rotor modes (for example, refer to Figure 10) are those modes in which the vibration is primarily confined to the rotating shaft. The participation of the pump column (casing) is minimal. These are the modes that could be found using a simple single-level model consisting of only the rotor and bearings.

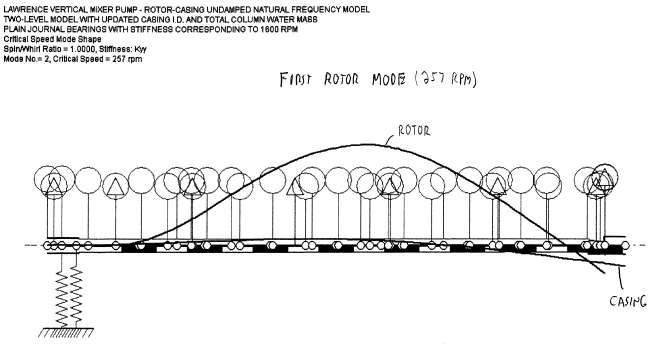

Figure 10. First Rotor Mode (257 rpm) with Plain Cylindrical Bearings.

- On the other hand, casing modes are those in which the primary motion is occurring in the pump column. The rotor may also be vibrating (for example, refer to Figure 9) but its movement is a direct result of the casing's vibration. The uncovering of these casing modes is a direct benefit of the employment of a two-level model for this analysis. If the traditional single-level model had been employed, these modes would have remained undetected.

- Using the above two categories, the critical speeds can be divided up as follows:

  - Rotor modes: 257, 328, 493, 580, 861, 1255, 1653, and 1911 rpm

  - Casing modes: 55, 382, 1056, and 1980 rpm

- The mode shapes are all consistent with expectations. For instance, the first rotor mode at 257 rpm (refer to Figure 10) shows the rotor bending into a half sine wave. The second rotor mode at 328 rpm is characterized by a mode shape (not shown) that looks like a full sine wave. Likewise, all higher rotor modes contain one more half sine wave than the mode that preceded them.

- Similarly, the casing modes are seen to be consistent with conventional beam theory. The pump column, which is cantilevered at its top end at the motor stand mounting flange, is seen to behave similarly to a vibrating cantilever beam. The first mode at 55 rpm is seen to be a classic cantilever beam mode. It is also seen that the links between the pump column and the pump shaft at the nine journal bearings cause the rotor to be carried along with the pump column as it vibrates. Furthermore, the second casing mode at 382 rpm looks like a half sine wave, the third casing mode at 1056 rpm looks like a full sine wave, etc. The excellent agreement of both the rotor and casing mode shapes with expectations lends considerable credibility to the analysis results.

- Additional credibility is provided to the analysis by comparison of its predicted casing natural frequencies with those obtained from impact tests on the actual units. These impact tests repeatedly showed that the pump column has natural frequencies in the vicinity of 300, 900, and nearly 1800 cpm. Since the model found casing modes at 382, 1056, and 1980 rpm, the agreement is seen to be reasonably good. However, comparing the casing modes predicted by this analysis, in which the shaft is assumed to be rotating, with the test results is not strictly valid since the rotor was stationary when the impact tests were performed. In order to simulate this condition, another analysis was run in which the rotor was held stationary. For this analysis, the cognizant casing modes were found to occur at 335, 939, and 1737 rpm. Upon reviewing these results, the authors concluded that the excellent agreement

between the analysis and testing completely validated the analytical model.

- The large number of rotor modes observed in the vicinity of and below the 1600 rpm operating speed represent many potential rotordynamics problems since all these modes have to be passed through during startups and shutdowns. Additionally, the presence of these modes means that this unit is likely to be susceptible to rotordynamic instability via subsynchronous whirling. The presence of so many modes in this speed range is due to the use of plain cylindrical journal bearings in a vertical installation. Since these bearings can only develop a significant stiffness if they are subjected to a radial load and since the vertical orientation results in the radial loadings being minimal, the bearing stiffnesses are alarmingly low. In the authors' and many other experts' experience, this is fairly typical of these types of machines and provides a strong justification for not utilizing plain cylindrical journal bearings in vertical pumps.

Stability Analysis

It was, therefore, determined that there are several modes of concern that lie within or beneath the operating speed range. The existing machine's ability to withstand these modes was then evaluated via a damped natural frequency/stability analysis. The authors analyze rotor-bearing stability by calculating the system's complex eigenvalues. The imaginary part of the eigenvalue is the damped natural frequency while the real part is known as the amplitude growth exponent. The more conventionally used logarithmic decrement is obtained directly from the growth exponent. Negative values of the log decrement indicate that a freely vibrating system's amplitudes will grow with time while positive values mean they will decay. Based on experience, the authors require that all modes demonstrate a log decrement of +0.30 or greater for machines, like this one, where nominal tolerance conditions are being considered.

The stability analysis was run with the same input parameters as the undamped natural frequency analysis except all eight stiffness and damping coefficients were input for all hydraulic supports. Additionally, since the damped natural frequencies are functions of operating speed, the 1600 rpm running speed was specified.

The pertinent results of the stability analysis are provided in Table 1. The table provides all the calculated damped natural frequencies and associated log decrements of interest. When the analysis was performed, both forward and backward whirling modes were uncovered, which is typical for any turbomachine. However, since there are no mechanisms present for exciting them, all the backward whirling modes were discarded from consideration. Accordingly, only the forward whirling modes are presented in the table.

Table 1. Stability Analysis Results with Plain Cylindrical Bearings.

DAMPED MODE NO.	Damped Natural Frequency (rpm)	LOG DEC.	MODE TYPE
1	55	-0.0036	Casing
2	347	-0.0089	Casing
3	645	-0.0447	Rotor
4	759	-0.0746	Rotor
5	764	-0.1253	Rotor
6	773	-0.2352	Rotor
7	790	-0.1684	Rotor
8	968	+0.0906	Casing
9	1798	+0.0849	Casing
10	2364	+0.0436	Rotor

Examination of the stability analysis results leads to the following observations and conclusions:

- As was found in the undamped analysis, the critical speeds can be broken down into two types of modes—rotor modes and casing modes—and are so identified in the table.
- Although there is not an exact one-to-one correspondence, most of the damped modes are seen to be related to the undamped modes in both the value of their critical speeds and the mode shapes.
- The first two casing modes, at 55 and 347 rpm, are both seen to have negative log decrements, supposedly indicating instability. This is not unusual since casing modes have a tendency to be very lightly damped. However, since the instability-producing mechanisms in this system—hydraulic forces at the bearings and impeller—are incapable of exciting casing vibrations, the casing modes are not a concern from a stability standpoint.
- However, it is also seen that there are numerous rotor modes (at 645, 759, 764, 773, and 790 rpm) that have negative log decrements. Their associated deflected shapes are provided in Figures 11 through 15. As was the case with the undamped mode shapes, the left end of the deflected shape plots represents the top end (motor/pump flexible coupling) of the model while the right end corresponds to the bottom end (pump impeller). These modes do represent problems and are almost certainly the reason that the current pumps with the plain cylindrical bearings have experienced numerous vibration problems and bearing and seal failures.

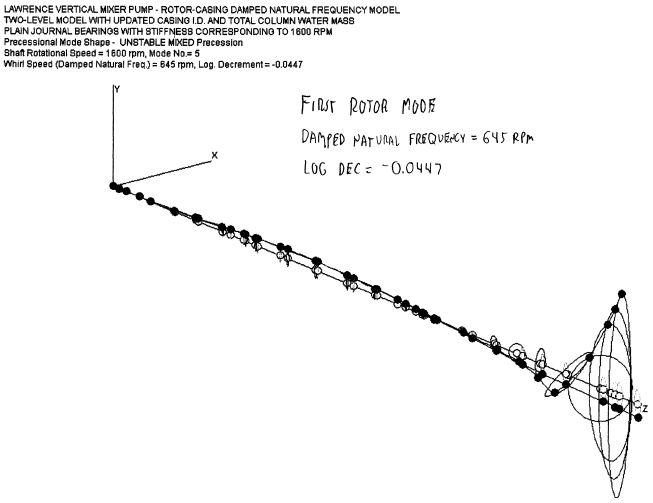

Figure 11. First Damped Rotor Mode (645 rpm) with Plain Cylindrical Bearings.

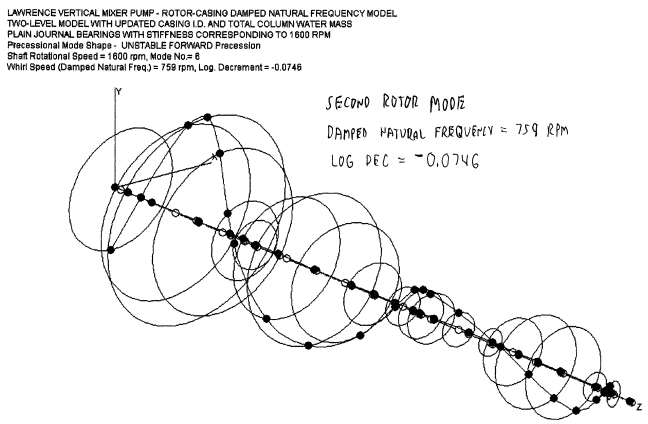

Figure 12. Second Damped Rotor Mode (759 rpm) with Plain Cylindrical Bearings.

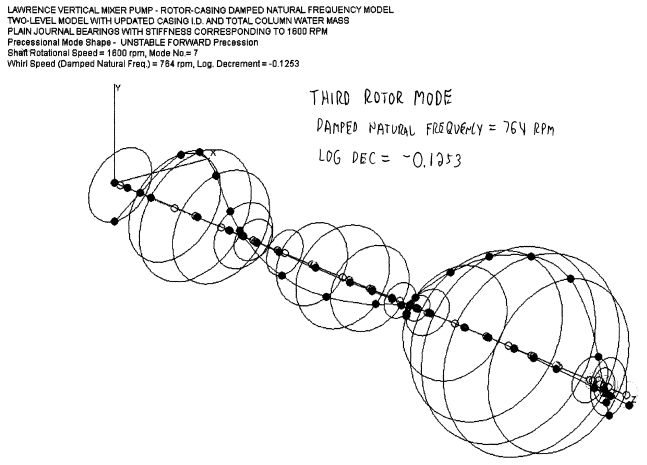

Figure 13. Third Damped Rotor Mode (764 rpm) with Plain Cylindrical Bearings.

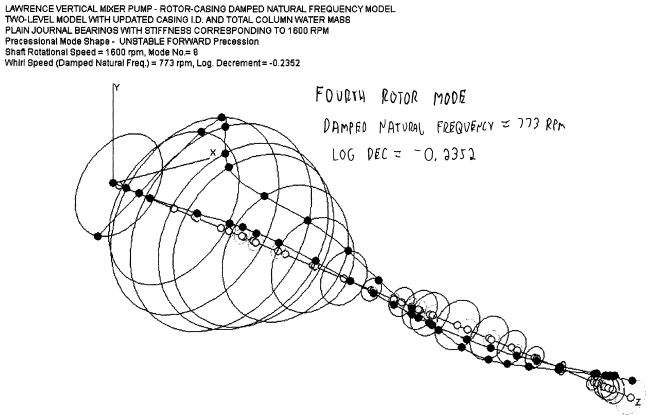

Figure 14. Fourth Damped Rotor Mode (773 rpm) with Plain Cylindrical Bearings.

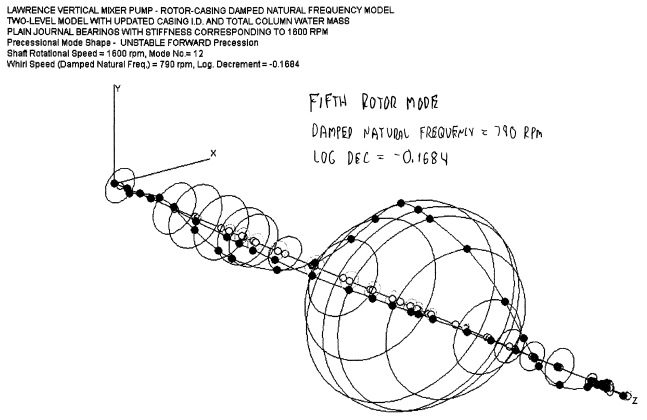

Figure 15. Fifth Damped Rotor Mode (790 rpm) with Plain Cylindrical Bearings.

After performing the stability analysis, the next task the authors would have normally undertaken is the performance of an unbalance response analysis to look at what happens when the critical speeds are traversed during startups and shutdowns. However, since the pump users informed the authors that these pumps have never experienced any vibration problems during startups or shutdowns, it was mutually agreed that this analysis could be omitted. Accordingly, performance of the stability analysis represented the culmination of the analysis of the initial pump with the plain cylindrical bearings.

In summary, the rotordynamics analysis has clearly revealed that the observed vibration problems with these pumps are due to unstable subsynchronous whirling. The large number of unstable rotor modes at speeds below one-half the 1600 rpm running speed will easily be excited by the cross-coupling in the plain cylindrical bearings. Furthermore, the primary cause of this instability is the employment of nonpreloaded, plain cylindrical journal bearings, whose virtually negligible stiffnesses give rise to the large number of rotor critical speeds below the 1600 rpm operating speed.

TILTING-PAD BEARING DESIGN

The rotordynamics analysis' confirmation that this pump was suffering from an instability problem confirmed what the authors had already suspected—that the employment of plain cylindrical bearings in this application was poor design practice. Accordingly, the authors then embarked on the design of a new set of tilting-pad bearings to replace the original water-lubricated plain cylindrical bearings. It was expected that the use of tilting-pad bearings employing offset pivots and geometric preload would correct the fatal flaw in the original design—virtually zero stiffness and damping at the bearings due to the lack of external loading. Although making this change to the process-lubricated bearing would also likely result in improved rotordynamic performance, other considerations prevented this bearing from being changed.

The philosophy chosen for the design of these bearings was to carry over as many design features as possible from some liquid sodium-lubricated bearings that the authors recently designed for a similar vertical pumping installation. Those bearings have been observed to perform flawlessly when lubricated with both water and liquid sodium. Since the design considerations for water-lubricated bearings are similar to those for liquid sodium bearings (both fall under the realm of process-fluid lubricated bearings), the liquid sodium bearings were a good starting point for the design of these bearings. Accordingly, the design parameters that were selected are as follows:

- *Bearing type*—Four-pad tilting-pad bearing oriented such that the maximum load acts between the pivots. This is the exact same bearing type as was used in the liquid sodium project. Some of the advantages of utilizing the tilting-pad design include the following:

  - Provides bearing misalignment compensation that, in the authors' experience, is important in water-lubricated bearings. Their experience with water-lubricated bearings is that some form of self-alignment feature is needed to ensure maintenance of a full fluid-film. This is because such applications necessitate the use of hard materials on both shaft and bearing that foregoes the forgiveness provided by soft materials such as babbitt and carbon. Employment of a tilting-pad bearing with a spherical seat in this design ensures that the bearing surfaces always remain parallel to the shaft, a paramount requirement for these types of bearings.

  - Provides much better rotordynamic performance than do plain cylindrical journal bearings since this bearing provides a significant stiffness to support the rotor (by virtue of the use of preloading and offset pivots) even when it is completely unloaded

  - Greatly reduces the pump's susceptibility to rotordynamic instability because its cross-coupling stiffness coefficients are essentially zero

  - Provides better capability for operating at small film thicknesses, which are an inherent feature of water-lubricated bearings, by virtue of the pads' abilities to move. In fixed-pad bearings operating at small film thicknesses, a momentary disturbance can easily cause a damaging touch-down. Conversely, in tilting-pad bearings, since the tilting pads are not rigid, such a disturbance is nowhere near as likely to generate contact since the

pads are free to momentarily deflect in response to the shaft's motion and then return to their steady-state positions.

- *Pad arc*—80 degrees—Same as liquid sodium bearing

- *Diameter*—2.50 inches—This is one area where deviation from the liquid sodium design was necessary since this pump's shaft dictates the use of a 2.50 inch diameter bearing.

- *Length*—2.50 inches—The authors' experience with water-lubricated tilting-pad bearings is that the optimum length-to-diameter ratio lies in the range between 0.70 and 1.00. The selected ratio of 1.0 is, therefore, consistent with this.

- *Machined clearance ratio*—1.5 mils per inch of diameter – The authors' experience with water-lubricated bearings is that the optimum clearance ratio lies within the range from 1.5 to 2.0 mils per inch of diameter. Since preliminary calculations revealed that use of the 1.5 ratio yielded a substantial improvement in rotordynamic performance (higher direct stiffness and damping coefficients) compared to the 2.0 ratio, this was the ratio selected for this bearing.

- *Preload ratio*—0.40—The advantage of preloading the bearing is that it ensures that all the pads are loaded even when there is no load on the bearing. This eliminates the potential problems of pad flutter and spragging, which can occur in nonpreloaded tilting-pad bearings. Additionally, as stated earlier, preloading the bearing guarantees that the bearing will generate a significant stiffness even in the unloaded condition, a significant benefit from a rotordynamics standpoint. Preliminary calculations revealed that the 0.40 ratio, combined with the 1.5 mils per inch clearance ratio, would yield the optimum rotordynamic characteristics.

- *Pivot offset ratio*—0.55—It is the authors' experience that in unidirectional rotation applications, tilting-pad bearings perform better when their pivot point is located closer to the pad's trailing edge than its leading edge. The reason for this is that the resultant load-carrying converging wedge is larger than for a centrally-pivoted design. Additionally, like preloading, utilization of offset pivots ensures that all pads are loaded even when the net load on the bearing is zero. The 0.55 ratio is identical to that used on the liquid sodium bearing.

Once the preliminary design parameters were selected, the authors utilized their proprietary procedure for evaluating the performance of process fluid-lubricated bearings to predict the minimum film thickness for the most highly-loaded tilting-pad bearing. Since the primary radial load acting on these bearings is that generated by the asymmetric pressure distribution at the pump impeller, the bottom tilting-pad bearing will be, by far, the most heavily loaded due to its proximity to the impeller. The maximum radial load acting on this bearing was approximated using the standard Hydraulic Institute procedure for a double volute impeller to calculate the impeller's radial load. Using this calculated load, the minimum film thickness at the pivot was determined to be 0.60 mils. Since the authors' water-lubricated bearing experience dictates that the calculated pivot film thickness should exceed 0.50 mils, it is seen that this bearing's steady-state performance should be fully satisfactory.

Once the tilting-pad bearings' steady-state performance had been determined, the authors calculated their rotordynamic stiffness and damping coefficients using a procedure similar to that previously described for the plain cylindrical bearings. As had been done for the lowest water-lubricated plain cylindrical bearing, the radial load acting on the bottom tilting-pad bearing was assumed to arise entirely from the impeller's radial thrust. Additionally, in order to simplify the model, all the other tilting-pad bearings were assumed to be unloaded. This is a conservative assumption since the unloaded condition yields the minimum stiffness and damping coefficients and, thereby, represents the worst case from a rotordynamics standpoint.

ROTORDYNAMIC ANALYSIS OF PUMP WITH TILTING-PAD BEARINGS

Undamped Critical Speed Analysis

The results of the rotordynamic analysis of the plain cylindrical bearing system were encouraging since they suggested that the proposed change to preloaded tilting-pad bearings would probably correct the uncovered instability problems. Accordingly, the next task undertaken was the analysis of the new system with the top eight bearings switched from plain cylindrical to tilting-pad bearings.

Once again, the first analysis run for the new configuration was the undamped critical speed analysis. The tilting-pad bearing coefficients for the planned operating speed of 1600 rpm were input to the rotordynamics code and undamped natural frequency analysis was run. Since four-pad tilting-pad bearings with the load between the pivots have perfectly symmetric stiffness and damping coefficients (i.e., $k_{xx} = k_{yy}$), once again, only one set of critical speeds needed to be generated.

The undamped critical speeds for the modified pump were, thereby, calculated to be 55, 345, 936, 1248, 1859, and 2349 rpm. Examination of the corresponding mode shapes (not shown) leads to the following observations and conclusions:

- Changing from plain cylindrical bearings to tilting-pad bearings has only a minor impact on the casing modes. In general the casing mode critical speeds, which were at 55, 382, 1056, and 1980 rpm, have decreased slightly (to 55, 345, 936, and 1859 rpm). Examination of the respective mode shapes reveals why this shift has occurred. With the tilting-pad bearings, the high resulting stiffnesses make the bearings behave as rigid connections and, as a result, the rotor is forced to follow the pump column's motion almost exactly. With the plain cylindrical bearings, although the column's motion generates motion in the rotor, the rotor's mode shape is allowed to deviate significantly from the column's due to the low stiffnesses provided by the plain cylindrical bearings. As a result of this, the casing sees a higher effective mass in the tilting-pad bearing system (since it is forced to carry the rotor along with it), and thus, that system's natural frequencies are lower.

- Introduction of the tilting-pad bearings has had the desired effect on the system since the much higher stiffnesses they provide has resulted in the large number of rotor modes that were previously below the 1600 rpm operating speed being raised to values somewhere above the operating speed. In fact the only rotor mode below the operating speed in the new system is the mode at 1248 rpm, whose mode shape is provided in Figure 16, which is primarily characterized by motion at the impeller and at the process fluid-lubricated bearing. If this bearing could also have been changed to a tilting-pad design, this mode would also have almost surely risen above the operating speed. However, since that was not a viable option, the decision was made to leave that mode as-is and try to verify that it would not create any problems via the stability analysis.

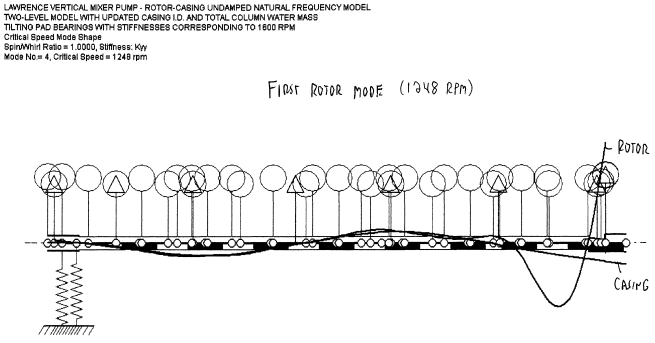

Figure 16. First Rotor Mode (1248 rpm) with Tilting-Pad Bearings.

Stability Analysis

Once the undamped analysis for the new machine was completed, a stability analysis was run in the same manner as that for the existing design. The results of this analysis are provided in Table 2. Once again, the only modes that are reported are those for which the whirling direction is forward.

Table 2. Stability Analysis Results with Tilting-Pad Bearings.

DAMPED MODE NO.	Wd (RPM)	LOG DEC.	MODE TYPE
1	55	-0.0010	Casing
2	347	-0.0041	Casing
3	775	+0.6104	Rotor
4	963	+0.0466	Casing
5	1793	+0.0524	Casing
6	2358	+0.0159	Rotor

Examination of the table reveals that, once again, the casing modes have either negative or small positive log decrements. However, since there is no mechanism capable of exciting these modes subsynchronously, they are not of concern. The primary mode of interest is the first rotor mode at 775 rpm, whose deflected shape is provided in Figure 17. However, from the figure, it is seen that this mode has a log decrement of +0.6104, which means that it should be well-damped and stable. Although the second rotor mode has a fairly small log decrement (+0.0159), its critical speed of 2358 rpm is far enough above the 1600 rpm operating speed to render it inconsequential. Thus, the new system is concluded to be fully satisfactory from a stability standpoint.

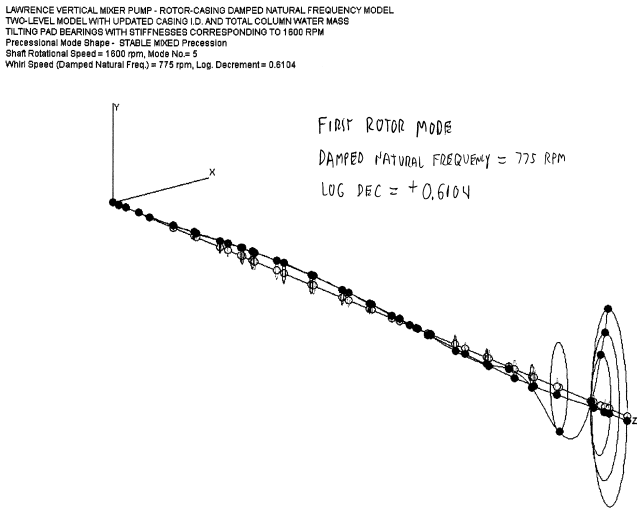

Figure 17. First Damped Rotor Mode (775 rpm) with Tilting-Pad Bearings.

The completion of the stability analysis represented the completion of the analytical activity for the new machine with the tilting-pad bearings. The analytical results have shown that the decision to switch to tilting-pad bearings is a good one and that the new configuration should not experience any vibration problems when run at 1600 rpm.

RETROFIT OF PUMP WITH TILTING-PAD BEARINGS

To implement the bearing retrofit program, the pumps were disassembled to permit removal of the plain cylindrical bearings from the bearing housings. The bearing housings were then remachined to accommodate the tilting-pad bearings. The tilting-pad bearings were fabricated and installed in the bearing housings by the bearing manufacturer. The bearing assemblies, one of which is shown in Figure 18, were then installed in the pumps and the pumps were retested for vibration.

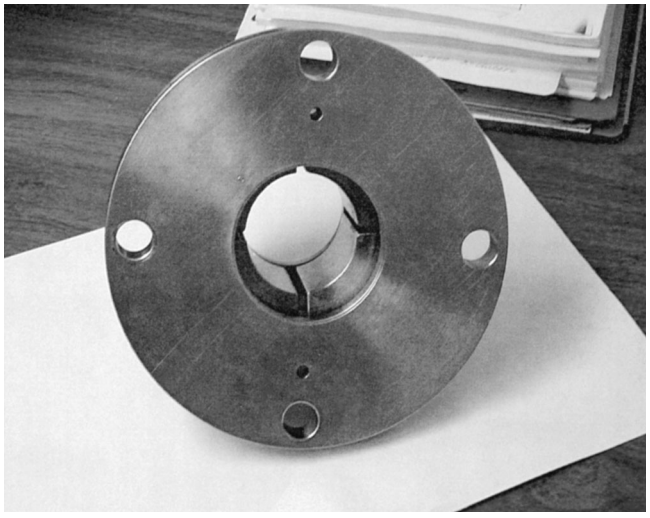

Figure 18. Tilting-Pad Bearing Assembly.

The vibration tests, whose results at the same locations as those of Figures 7 and 8 are presented in Figures 19 and 20, respectively, clearly demonstrated the substantial benefits reaped by making the bearing change. The data indicate that the ½× vibration is virtually eliminated along the shaft between the tilting-pad bearings, and it is also nearly eliminated near the impeller where the shaft is supported by one tilting-pad bearing and the process-lubricated journal bearing. This elimination of the subsynchronous vibration should result in drastic improvements in both bearing and seal life.

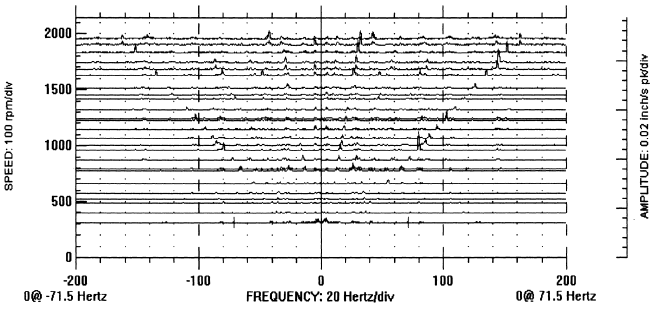

Figure 19. Mid-Span Accelerometer Measured Vibrations for Modified System.

Two consecutive tests were performed to validate the pump's performance after the tilting-pad bearings were installed. A preliminary, 288 hour, pump test was performed, and a 72 hour acceptance test followed. Each of these tests was performed at 1600 rpm, which results in over 27 million cycles. Since cyclic

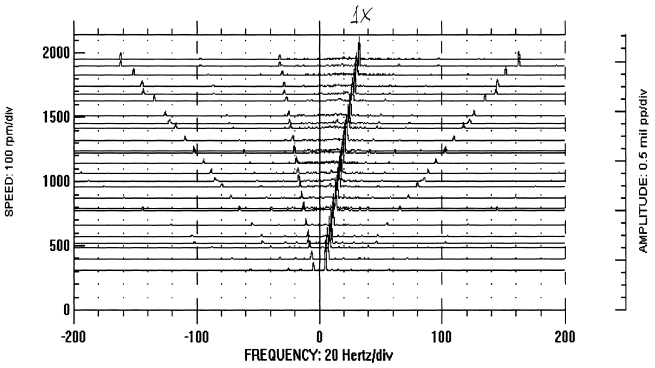

Figure 20. Proximity Probe Measured Vibrations for Modified System.

failures due to fatigue generally do not occur in metals above one to 10 million cycles, this test duration was expected to identify all fatigue failures. Thorough disassembly and inspection of parts were performed after the preliminary test. No signs of any distress in any of the parts were uncovered. Accordingly, the change to the tilting-pad bearings was concluded to have completely solved this pumping system's vibration whirl problems.

CONCLUSION

The presented case study has shown how both experimental vibration analysis and rotordynamics analysis can be effectively used to solve practical field problems. The most important lessons that should be retained from this study are as follows:

- A thorough lateral rotordynamics analysis should always be included as an integral part of the design process for any vertical pump.
- Although there are some people who consider rotordynamic analysis to be an academic curiosity, when performed correctly, it can quickly and efficiently identify the causes of field problems and evaluate a number of potential corrective actions.
- In order to accurately analyze a vertical pump having a flexible casing, such as this one, the rotordynamics analysis must be conducted using a multilevel model. The popular belief that a general purpose finite element code can be used for such analyses is totally inaccurate unless the fluid-structure-interaction connections between the rotor and casing are properly accounted for.
- Although rotordynamic analysis is an effective tool by itself, it is much more effective, as was the case here, when it is combined with experimental vibration analysis. It is important that the rotordynamic analysis' predictions match the observed results, as was the case for the pump column's natural frequencies in this system. If a deviation is found, the rotordynamic model should be tweaked until its predictions match reality.
- In most cases, the use of plain cylindrical bearings in vertical pumping applications is just plain bad design and is highly likely to lead to vibration problems. A much better choice is to use some type of preloaded bearing, with a tilting-pad bearing being the optimum choice.
- Rotordynamics analysis is not an exact science that can be performed by just anybody. The importance of the skill, judgment, and experience of the analyst should never be underestimated.

REFERENCES

Berzatzy, P. G., Hsing, F. C., Lund, J. W., and Malanoski, S. B., 1972, "Dynamic Evaluation of FFTF Sodium Pump and Fluid Coupling Test Model," MTI Report 72TR1, Mechanical Technology Incorporated, Latham, New York.

Chang, C. M. and Braun, F. W., 1987, "Solving the Vibration Problem of a Vertical Multistage Cryogenic Pump," *Proceedings of the Fourth International Pump Symposium*, Turbomachinery Laboratory, Texas A&M University, College Station, Texas, pp. 85-95.

Chen, H. M., Malanoski, S. B., and Lewis, P., 1978, "Dynamic Analyses of Salt Pumps," MTI Report 78TR104, Mechanical Technology Incorporated, Latham, New York.

Childs, D. W., 1978, "The Space Shuttle Main Engine High-Pressure Fuel Turbopump Rotordynamic Instability Problem," ASME Journal of Engineering for Power, pp. 48-57.

Childs, D. W., 1993, *Turbomachinery Rotordynamics—Phenomena, Modeling, and Analysis*, New York, New York: John Wiley & Sons, Inc.

Corbo, M. A. and Malanoski, S. B., 1998, "Pump Rotordynamics Made Simple," *Proceedings of the Fifteenth International Pump Users Symposium*, Turbomachinery Laboratory, Texas A&M University, College Station, Texas, pp. 167-204.

Crandall, S. H., 1982, "A Heuristic Explanation of Journal Bearing Instability," Proceedings of the Workshop on Rotordynamic Instability Problems in High-Performance Turbomachinery, Texas A&M University, College Station, Texas, pp. 274-283.

Darlow, M. S. and Smalley, A. J., 1976, "Byron-Jackson CRBRP Pump Bearing Stability Analysis," MTI Report 76TR37, Mechanical Technology Incorporated, Latham, New York.

Darlow, M. S., Smalley, A. J., and Ogg, J., 1978, "Critical Speeds and Response of a Large Vertical Pump," ASME Paper 78-PVP-34.

Habets, L. G. and Smalley, A. J., 2000, "The Rotordynamic Integrity of a New Machine—A Vertical Hydraulic Turbine in Cryogenic Fluids," *Proceedings of the Eighteenth International Pump Users Symposium*, Turbomachinery Laboratory, Texas A&M University, College Station, Texas, pp. 51-58.

Hagg, A. C., 1946, "The Influence of Oil Film Journal Bearings on the Stability of Rotating Machines," ASME Journal of Applied Mechanics, pp. A-211-A-220.

Hagg, A. C. and Warner, P. C., 1953, "Oil Whip of Flexible Rotors," ASME Transactions, pp. 1339-1344.

Hori, Y., 1959, "A Theory of Oil Whip," ASME Journal of Applied Mechanics, pp. 189-198.

Hull, E. H., 1957, "Oil-Whip Resonance," ASME Transactions, pp. 1490-1496.

Jain, P. C. and Srinivasan, V., 1975, "A Review of Self-Excited Vibrations in Oil Film Journal Bearings," *Wear*, pp. 219-225.

Lund, J. W. and Saibel, E., 1967, "Oil Whip Whirl Orbits of a Rotor in Sleeve Bearings," ASME Journal of Engineering for Industry, pp. 813-823.

Mitchell, J. R., Holmes, R., and Byrne, J., 1965-66, "Oil Whirl of a Rigid Rotor in 360 Degree Journal Bearings: Further Characteristics," Proceedings of the Institution of Mechanical Engineers, pp. 593-610.

Myrick, S. T. and Rylander, H. G., 1976, "Analysis of Flexible Rotor Whirl and Whip Using a Realistic Hydrodynamic Journal Bearing Model," ASME Journal of Engineering for Industry, pp. 1135-1144.

Newkirk, B. L. and Lewis, J. F., 1956, "Oil Film Whirl—An Investigation of Disturbances Due to Oil Films in Journal Bearings," ASME Transactions, pp. 21-27.

Newkirk, B. L. and Taylor, H. D., 1924, "Shaft Whipping Due to Oil Action in Journal Bearings," General Electric Review, pp. 559-567.

Orbeck, F., 1958, "Theory of Oil Whip for Vertical Rotors Supported by Plain Journal Bearings," ASME Transactions, pp. 1497-1502.

Pan, C. H. and Sternlicht, B., 1963, "Comparison Between Theories and Experiments for the Threshold of Instability of Rigid Rotor in Self-Acting, Plain Cylindrical Journal Bearings," ASME Paper 63-LubS-3.

Poritsky, H., 1953, "Contribution to the Theory of Oil Whip," ASME Transactions, pp. 1153-1158.

Rentzipis, G. M. and Sternlicht, B., 1962, "On the Stability of Rotors in Cylindrical Journal Bearings," ASME Journal of Basic Engineering, pp. 521-532.

Smalley, A. J., Hollingsworth, J. R., Habets, G. L., and Kimmel, H. E., 1998a, "Rotor Dynamic Analysis of a Cryogenic Submerged Turbine Generator," Proceedings of the Nineteenth Southeastern Conference on Theoretical and Applied Mechanics, SECTAM XIX, Deerfield Beach, Florida, pp. 708-718.

Smalley, A. J., Hollingsworth, J. R., Habets, G. L., and Kimmel, H. E., 1998b, "Rotor Dynamic Analysis of a Submerged Turbine Generator Driven by Liquefied Natural Gas," Proceedings of the Fifth International Conference on Rotor Dynamics, IFToMM, Darmstadt University of Technology, Darmstadt, Germany, pp. 298-309.

Tolle, G. C. and Muster, D., 1969, "An Analytic Solution for Whirl in a Finite Journal Bearing with a Continuous Lubricating Film," ASME Journal of Engineering for Industry, pp. 1189-1195.

Walter, T. J. and Zelingher, S., 1989, "Vibration Assessment of Variable Speed Vertically Mounted Pumps," *Proceedings of the Sixth International Pump Users Symposium*, Turbomachinery Laboratory, Texas A&M University, College Station, Texas, pp. 17-22.

ACKNOWLEDGEMENTS

The authors would like to recognize the contributions of Charley Sharpe, Brannen Adkins, and Bill Van Pelt of Westinghouse Savannah River, and Rich Armentrout and Stan Malanoski of No Bull Engineering, who all played prominent roles in helping to solve this troublesome problem. We would also like to thank Dr. Dara Childs and Vinod Patel of the Pump Symposium Advisory Committee for their invaluable feedback and encouragement.